Feasibility of optically detected cyclotron resonance to study electron mobility in ultrapure GaAs

M. Kozhevnikov
Division of Engineering and Applied Sciences, Harvard University, 9 Oxford Street, Cambridge, Massachusetts 02138
(Received 12 April 2000)

While the optically detected cyclotron resonance (ODCR) technique is a widely applied technique for the study of semiconductors, the effect of cyclotron resonance (CR) on the carrier capture and recombination processes is not well understood. We report on a comparative study of microwave CR and ODCR in photoexcited ultrapure GaAs at low temperatures. We found that the ODCR spectrum is broader and thus gives lower electron mobility than the CR spectrum under the same experimental conditions. To explain the discrepancy, a rate-equation model is developed for the dependence of the exciton density on the microwave power (free-electron temperature) under the CR conditions. A good agreement between the experimental data and the model calculations was obtained by assuming the exciton formation rate dependence on the hot-electron temperature.

I. INTRODUCTION

The optically detected cyclotron resonance (ODCR) technique is a widely applied extension of the conventional cyclotron resonance (CR) technique for study of semiconductors. In ODCR, the photoluminescence (PL) amplitude change by applied microwave (mw) or far-infrared (FIR) power is monitored as a function of the frequency or magnetic-field strength. In conventional CR experiments, the direct mw or FIR absorption of the whole sample is measured, and therefore it can be difficult to distinguish between the contribution from different structures presented in one sample. Thus, to study layered structures, it can be advantageous to use ODCR where the effect of the applied mw or FIR radiation on specific PL bands is measured. In some cases, ODCR gives even longer momentum relaxation times than those obtained CR in the dark, due to the photoneutralization of ionized impurities by photoexcited free carriers.[1–3] In addition, the mw or FIR absorption of carriers under CR conditions can lead to a selective triggering or quenching of different recombination processes, thus giving an enhanced optical resolution compared to photoluminescence measurements. The ODCR technique was successfully applied to study the band parameters (effective mass and mobility) in bulk semiconductors[4,5] and semiconductor nanostructures,[6–8] as well as to study recombination mechanisms[3,9–11] and quantum oscillations.[8,10,12,13]

In most cases, the ODCR is studied at FIR frequencies in the quantum limit, where a high magnetic field is used in order to study bulk and nanostructured semiconductors, usually with relatively low mobility.[4,12,14–16] In contrast, a CR/ODCR study at microwave frequencies requires low magnetic fields ($B<1$ T).[5,11,17,18] This experimental condition is termed ''classical'' CR/ODCR, as the carrier transport can be described by a classical equation of motion. It has a number of distinctions from the FIR CR/ODCR case (usually requiring $1<B<20$ T), where the carrier Landau quantization is important, and the scattering processes are affected by the magnetic-field strength.[19,20]

Several mechanisms are usually considered to explain the effect of the free-carrier heating by mw (FIR) power on the PL modulation:[3,7] (i) carrier trapping rate dependence on the carrier temperature, (ii) impact ionization of bound-carriers by hot free carriers, and (iii) thermal coupling, where the accelerated free carriers release their energy to the lattice which affects the PL. Which of the above ODCR mechanisms is dominant depends strongly on the nature of the PL transition monitored and on the experimental conditions.[3] For example, the threshold dependence of the PL signal on the mw power applied was observed in the case of modulation-doped GaAs/AlGaAs heterostructures, and it was interpreted in terms of the impact ionization mechanism.[21] Similarly, mw and FIR ODCR was studied in epitaxial InP and GaAs, and the effect of donor-bound exciton PL quenching was attributed to the bound-exciton impact ionization by hot electrons generated at CR conditions.[2,22] In contrast, in doped GaAs/$Al_xGa_{1-x}As$ quantum wells,[7] the threshold mw field indicative of the impact ionization mechanism was not observed, and it was concluded that the underlying physical mechanism of mw-modulated PL is a thermal heating of the lattice (the mw-modulated PL spectral shape is the temperature derivative of the PL spectrum). In photoexcited undoped GaAs/$Al_xGa_{1-x}As$ quantum wells[23] and bulk GaAs and CdTe,[24] the excitonic PL quenching by the intense FIR radiation was attributed to carrier heating without significantly heating the lattice. Smooth reduction of the free-exciton luminescence was observed in pure GaAs (with impurity concentration $N_I \sim 6\times10^{13}\,\mathrm{cm}^{-3}$) under an applied mw field, and it was attributed to the reduction of the exciton formation rate, while the impact ionization of free excitons is feasible at high mw and excitation powers.[22]

The expression for the mw (FIR) power absorption [see Eq. (4) below] is frequently used to describe the ODCR line shape in order to estimate the carrier effective mass and its mobility.[3,5,7,24] However, the ODCR measurements provide only indirect information on the transport properties of photogenerated charged carriers since the exciton photoluminescence modulation is monitored in the ODCR and not the direct mw (FIR) power absorption. Discrepancies between the CR and ODCR line shapes were observed in several experiments.[7,22,25,26] While the discrepancy between the mobilities extracted from the ODCR and from the magne-

totransport and Shubnikov–de Haas measurements on $GaAs/Al_xGa_{1-x}As$ quantum wells was explained by differences in the experimental conditions (carrier scattering may depend on the optical and mw (FIR) intensities),[7] our previous study of photoexcited mw CR/ODCR experiments in undoped bulk GaAs and GaAs/AlGaAs quantum wells show unambiguously that the carrier mobilities extracted from the simultaneously taken CR and ODCR linewidths are different.[25,26]

In this paper, we report on a study of the effect of carrier heating in the mw field on the recombination processes in ultrapure GaAs at low temperatures by using photoinduced mw CR and ODCR spectroscopy. We found that the excitonic photoluminescence spectra weaken gradually under applied mw irradiation, and this PL quenching is most efficient at the CR conditions. The ODCR spectrum monitored at the free exciton luminescence band is broader than the CR spectrum under the same experimental conditions. In order to gain a better understanding of the optical and transport properties, a model based on the main dissociation and generation-recombination processes governing electron and exciton dynamics is developed, and it explains well the observed results in terms of the exciton formation rate dependence on carrier temperature.

This paper is laid out as follows: In Sec. II, the experimental setup, the samples used and the experimental results are presented. In Sec. III we present the rate equation model for the photoexcited exciton and unbound electron densities, and analyze the experimental and model data.

II. EXPERIMENTAL PROCEDURE AND RESULTS

Ultrapure 10-μm GaAs layers were grown by vapor phase epitaxy (sample *A*) and molecular-beam epitaxy (sample *B*). From our previous study,[25] we estimated the electron mobility to be $\sim 2\times10^6\,\mathrm{cm^2/V\,s}$ in the purest sample *A* (with residual impurity concentration $N_I \sim 1.5\times10^{13}\,\mathrm{cm^3}$) and $\sim 0.9\times10^6\,\mathrm{cm^2/V\,s}$ in sample *B* ($N_I \sim 3\times10^{13}\,\mathrm{cm^{-3}}$) at $T_L = 2.2\,\mathrm{K}$. The samples were placed at the antinode of the mw electric field in an 8-mm waveguide mounted in an immersion-type dewar. A stabilized, 35.6-GHz Gunn diode was used as the mw source. The incident mw power P_{mw} was continuously varied by an electrically controlled attenuator so that the power incident on the sample was in the range of $P_{\mathrm{mw}} = 10^{-4} - 50\,\mathrm{mW}$. The mw radiation measured by the diode detector was modulated by the photoexcitation of the sample and the modulation signal was proportional to the photoinduced mw absorption (PMA) by the photoexcited free electrons. For cyclotron resonance measurements, an external dc magnetic field **B** was applied parallel to the [001] direction and was swept over the range 0–1 T (the mw electric field was polarized perpendicularly to **B**). The sample was illuminated by laser light (from a He-Ne or a tunable dye laser) through a pinhole in the waveguide. The photoluminescence (PL) signal was measured simultaneously with the PMA signal.

Figure 1 presents the PL spectra (in the exciton region) of samples *A* and *B* at $P_{\mathrm{mw}} = 0$. The PL spectra consist of free exciton (exciton polariton) (X) and excitons bound to neutral donor (D^0,X), ionized donor (D^+,X), and neutral acceptor (A^0,X). The free exciton band is the dominant band among

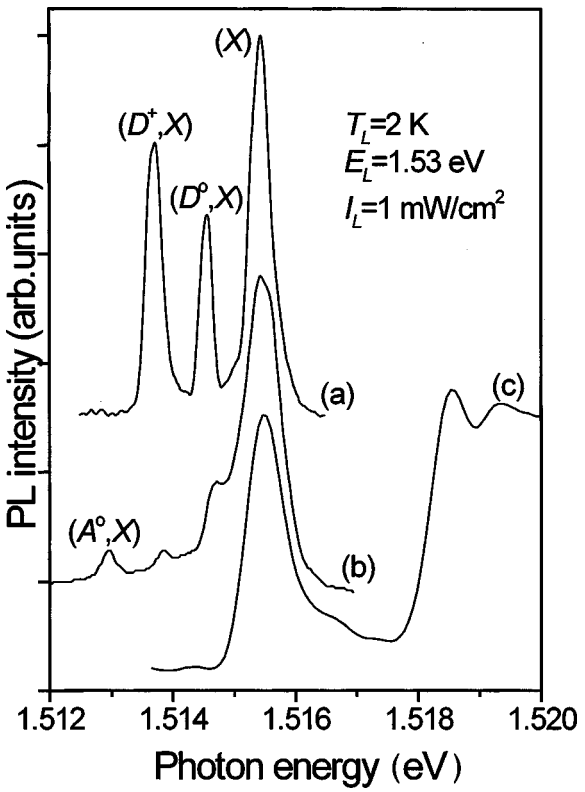

FIG. 1. The low-temperature photoluminescence spectra of (a) sample *A* and (b) sample *B*. (c) For comparison, the PL excitation spectrum of sample *B*, monitored at 1 LO-phonon sideband (PSB) of free exciton band is also shown.

the no-phonon excitonic transitions. For comparison, the PL excitation spectrum of sample *B* monitored at 1 LO-phonon sideband (PSB) of the free exciton band is also shown in Fig. 1. As was expected, there is no Stokes shift between the excitation and recombination spectra of the free exciton.

Under applied mw irradiation, we observed a strong quenching of the excitonic bands. Figure 2 shows the development of the excitonic and 1 LO-PSB PL signals of sample *A* for three values of incident mw power. While the free exciton PL band undergoes about a fourfold decrease at $P_{\mathrm{mw}} = 25\,\mathrm{mW}$, its linewidth remains essentially the same. In contrast, we observed a significant broadening of the 1 LO-PSB band as P_{mw} increases. By fitting the 1 LO-PSB line shape with the expression $(E-E_1)\exp\{-(E-E_1)/k_BT_{\mathrm{ex}}\}$,[27] where $E_1 = E_g - E_{\mathrm{ex}} - \hbar\omega_{\mathrm{LO}}$ and T_{ex} is the exciton temperature, we calculated that the exciton temperature increased to 5.6 K at $P_{\mathrm{mw}} = 25\,\mathrm{mW}$. Note that even at $P_{\mathrm{mw}} = 0$, the extracted $T_{\mathrm{ex}} = 3.6\,\mathrm{K}$ is above the bath temperature ($T_L = 2.2\,\mathrm{K}$) because of the effective exciton-hot electron interactions at above-band-gap excitation.[28] The exciton temperature increase does not show itself as a free exciton PL broadening because the radiative recombination of free excitons occurs only from luminescent states near the bottleneck region where excitonlike polaritons convert into photonlike polaritons.[29]

We compared the electron CR (PMA dependence on **B**) and ODCR (PL dependence on **B**) traces of both samples at $T_L = 2\,\mathrm{K}$ (for the same P_{mw} and I_L for each sample), as shown in Fig. 3. The ODCR trace was monitored at the free exciton band. The level of mw irradiation was kept to be

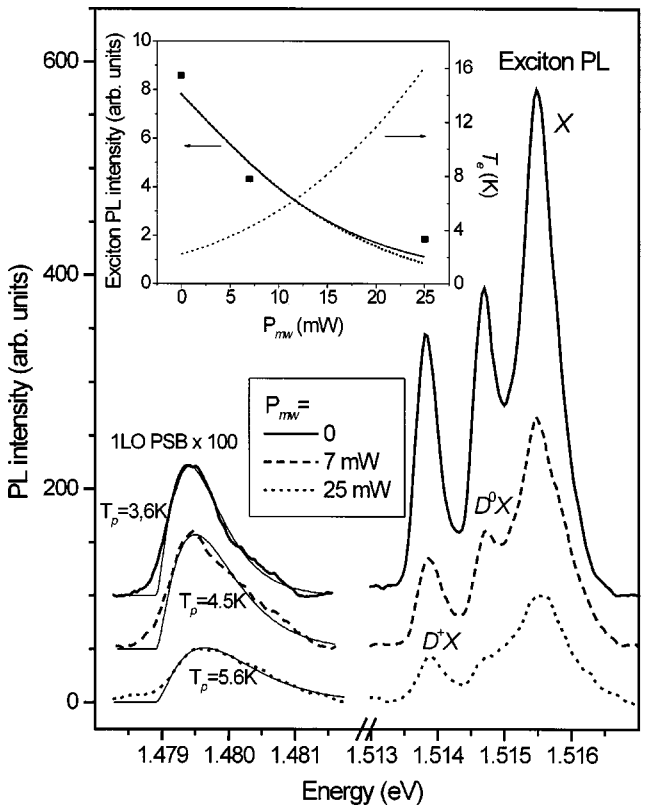

FIG. 2. The exciton PL and $(1\ \mathrm{LO})_X$ PSB spectra of sample A for three values of incident mw power at $T_L=2.2$ K and $I_L=10$ mW/cm^2. The exciton temperatures T_p, extracted from the $(1\ \mathrm{LO})_X$ PSB line shapes, are indicated near the fitting curves (thin solid lines). The inset shows the free exciton PL quenching (solid squares) as a function of the incident mw power. The calculated $n^0_{\mathrm{ex}}(P_{\mathrm{mw}})$ dependencies are shown for $\beta_0=10^{-5}$ cm^3 s^{-1} (solid line) and $\beta_0=3\times10^{-4}$ cm^3 s^{-1} (dotted line), and the $T_e(P_{\mathrm{mw}})$ dependence is shown by dashed line, using $N_I=1.5\times10^{13}$ cm^{-3} and $G=10^{20}$ photons/cm^3 s.

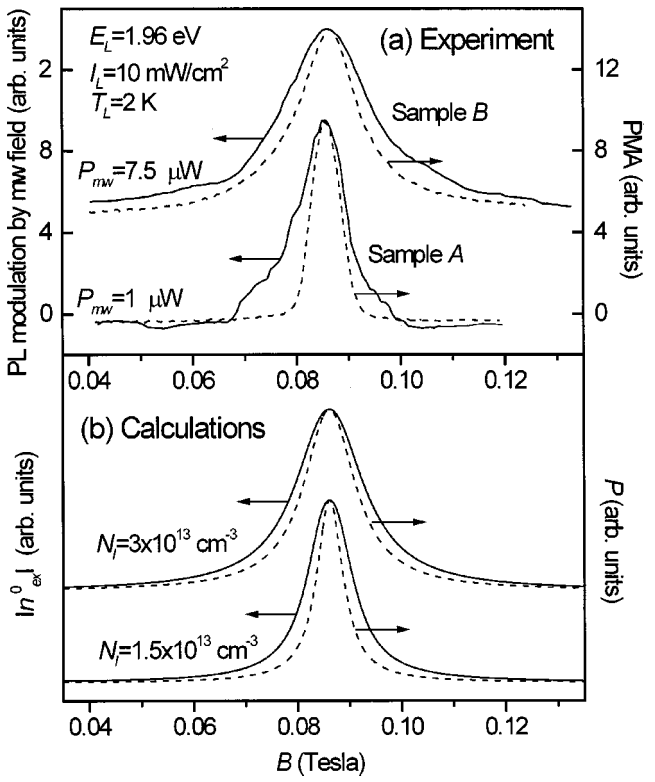

FIG. 3. (a) Experimentally observed normalized CR (dashed lines) and ODCR (solid lines) traces for both samples. The CR data were observed by direct monitoring the PMA signal, while the ODCR data were observed monitoring the free exciton PL band. (b) Calculated CR spectra [given by $P(B)$] and ODCR spectra [given by $|n^0_{\mathrm{ex}}|(B)$] for two impurity concentrations at $T_L=2$ K and $G=10^{19}$ photons/cm^3 s using model parameters of Table I.

extremely low (several μW) to eliminate nonlinear electron heating processes in CR spectra. One can see that for both samples, the ODCR spectrum is broader than the CR spectrum.

III. MODEL AND ANALYSIS

To analyze the experimental results, we use a rate equation model for the time evolution of the electron (n) and free exciton (n_{ex}) densities. This model includes the main generation-recombination and dissociation processes governing electron and free exciton dynamics[30,31] (for simplicity, the bound-exciton related transitions are implicitly included into the free exciton recombination time):

$$\frac{dn}{dt}=G-\gamma n^2+an_{\mathrm{ex}}+\beta n n_{\mathrm{ex}}-\frac{n}{\tau_1}, \tag{1a}$$

$$\frac{dn_{\mathrm{ex}}}{dt}=\gamma n^2-an_{\mathrm{ex}}-\beta n n_{\mathrm{ex}}-\frac{n_{\mathrm{ex}}}{\tau_2}. \tag{1b}$$

Here $G(E)=\alpha(E)I_L(E)/E$ is the free-electron generation rate at the above-band-gap photoexcitation (with energy E), where $\alpha(E)$ is the absorption coefficient. Excitons are formed at a rate of γn^2, where γ is the bimolecular exciton formation coefficient. $a=\gamma N\exp(-E_{\mathrm{ex}}/k_BT_L)$ is the exciton thermal dissociation coefficient, where N is the effective reduced density of states. The term $\beta n n_{\mathrm{ex}}$ describes the impact ionization rate of excitons by hot electrons, where β is the impact ionization coefficient. The electron and exciton total recombination rates are given by the terms n/τ_1 and n_{ex}/τ_2, where τ_1 and τ_2 are their respective recombination times. The model parameters used in the calculations are summarized in the Table I.

The steady-state solution of Eqs. (1), $(dn/dt=dn_{\mathrm{ex}}/dt=0)$, gives the following expressions for the exciton density:[32]

$$n^0_{\mathrm{ex}}=\tau_2G-\frac{\tau_2C_1}{2\tau_1C_2}\left[\sqrt{1+\frac{4G\tau_1C_2(1+\tau_2a)}{C_1^2}}-1\right], \tag{2}$$

where $C_1=\tau_2(a-\beta\tau_1G)+1$ and $C_2=\gamma\tau_1+\beta\tau_2$.

We assume that the main effect of the electron heating on the exciton density is due to γ and β dependences on the hot-electron temperature. Under electron heating, there are variations in the free-electron energy-distribution function, and the mean value of the electron energy E_e increases with the electric-field strength ε. Assuming that the hot electrons have a Maxwellian distribution function with an effective electron temperature $T_e=2E_e/3k_B$, β may be approximated

TABLE I. Parameter values used in the model calculations.

Parameter	This work	From references
Electron recombination time τ_1 (s)	1×10^{-7}	1×10^{-7} (Ref. 22) $\sim2\times10^{-6}$ (Ref. 32)
Exciton recombination time τ_2 (s)	5×10^{-9}	$(4-5)\times10^{-9}$ (Refs. 33 and 34)
Exciton impact ionization coefficient β_0 ($cm^3\,s^{-1}$)	10^{-5}	$\sim10^{-5}$ (Ref. 35) 2×10^{-4} (Ref. 22)
Exciton formation coefficient γ_0($cm^3\,s^{-1}$)	10^{-5}	$\sim5\times10^{-5}$ (Ref. 36) $\sim10^{-4}$ (Ref. 22) $10^{-7}-10^{-5}$ (Ref. 37)
Exciton binding energy E_{ex} (meV)	4.1	4.1 (Ref. 38)
$N=\left(\frac{2\pi m_e m_h k_B T_L}{h^2(m_e+m_h)}\right)^{3/2}$ (cm^{-3})	$2.7\times10^{13}T_L^{3/2}$	using $m_e=0.067\,m_0$ $m_h=0.2m_0$

by $\beta=\beta_0\exp(-E_{ex}/k_BT_e)$, where $\beta_0=\pi a_B^2\nu_e$, a_B is the exciton Bohr radius and ν_e is the electron velocity.[39] In contrast to β, γ decreases with the carrier temperature.[22,40,41] In our model, we adopt the $\gamma\sim T_e^{-3/2}$ dependence from Ref. 22 and write it in the form $\gamma=\gamma_0(T_L/T_e)^{3/2}$.

The electron temperature dependence on the electric-field strength ε can be found from the balance equation[42]

$$\frac{dT_e}{dt}=\frac{2}{3k_B}P(\omega,B)-\frac{T_e-T_L}{\tau_e}, \tag{3}$$

where τ_e is the energy relaxation time and $P(\omega,B)$ is the electric-field power absorbed per electron. In the case of linearly polarized microwave radiation with frequency ω, the microwave power absorption per electron due to its rotation in the magnetic field **B** is given in the classical case by[43]

$$P(\omega,B)=\frac{e^2\tau}{m^*}|\varepsilon(\omega)|^2\frac{1+(\omega^2+\omega_c^2)\tau^2}{[1+(\omega^2-\omega_c^2)\tau^2]^2+4\omega_c^2\tau^2}. \tag{4}$$

Here $\omega_c=eB/m^*$ is the cyclotron frequency, m^* and τ are the effective mass and momentum relaxation time (at microwave frequencies) of the charge carrier, respectively. The $P(\omega,B)$ dependence given by Eq. (4) is usually used to fit the experimentally observed CR traces in order to extract the carrier effective mass and its momentum relaxation time.[3] According to this expression, in order to observe a resonancelike CR trace, $\omega_c\tau\geqslant1$. Consequently, only samples with a very high carrier mobility can satisfy the mw CR condition $\omega_c\tau\geqslant1$ at low magnetic fields.

To solve Eq. (3) for T_e, the τ and τ_e dependencies on T_e should be considered. At $T_e<50$ K, the electron-energy relaxation is due to the electron-acoustic phonon and electron-ionized impurity scattering.[39] In pure GaAs, the electron-phonon interaction is dominant and is primarily via the piezoelectric potential. In this case, $\tau_e^{-1}=\tau_{pe}^{-1}(2m^*s^2/k_BT_L)$,[44] where τ_{pe} is the electron momentum relaxation time due to the electron-acoustic phonon interaction via the piezoelectric potential and s is a sound velocity ($s=4.73\times10^5$ cm/s in GaAs). From our previous study,[25] $\tau_{pe}^{-1}=5\times10^9T_L/T_e^{1/2}$, and, thus $\tau_e=bT_e^{1/2}$, where $b\approx10^{-9}\,K^{-1/2}$ s. The low-temperature electron mobility in undoped GaAs crystals with residual impurity concentration of $>10^{13}\,cm^{-3}$ is limited by neutral-impurity scattering with $\tau^{-1}=cN_I^{25}$, where c is a constant [$c=(4-8)\times10^{-4}\,cm^3\,s^{-1}$ from Ref. 25]. Since the electron-energy-relaxation rate is much larger than the rate of electron-density variation, we can approximate the electron temperature by the value obtained from the steady-state solution $dT_e/dt=0$:

$$T_e=T_L+\frac{K^2}{2}\left[1+\sqrt{1+\frac{4T_L}{K^2}}\right], \tag{5}$$

where $K=2bP(\omega,B)/3m^*$ with $\tau=(cN_I)^{-1}$.

Figure 4 shows the calculated T_e dependence on the magnetic field for several P_{mw} values at $T_L=2.2$ K (the incident mw power P_{mw} is related to the mw field strength ε by the standard expression for rectangular waveguide[45]). One can see that the resonance increase of T_e strengthens as P_{mw} increases. Note that at $\mathbf{B}=0$, T_e also increases with the P_{mw} increase, but this increase is much weaker than that at the CR condition.

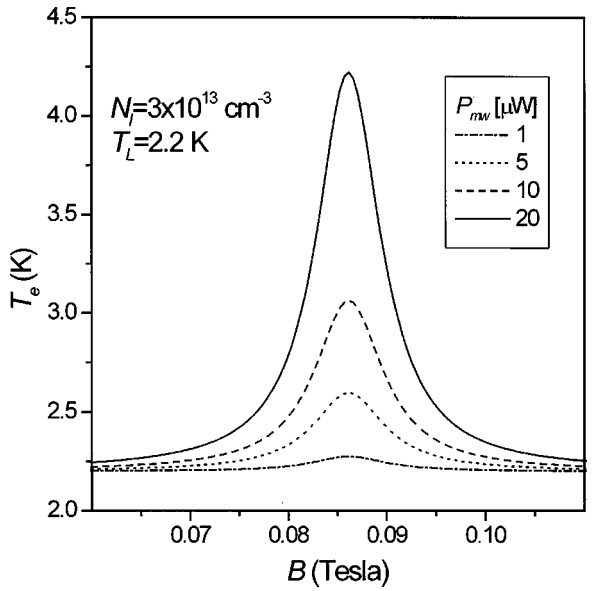

FIG. 4. The calculated electron temperature dependence on the applied magnetic-field strength for four applied mw powers, using $T_L=2$ K, $N_I=3\times10^{13}\,cm^{-3}$ and model parameters of Table I.

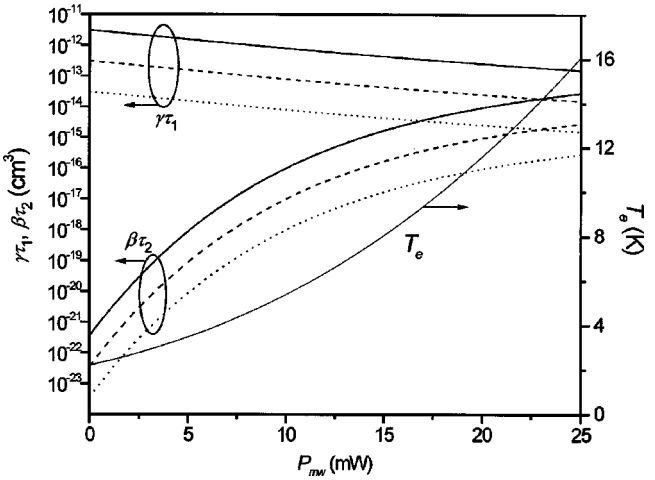

FIG. 5. The calculated $\gamma\tau_1$, $\beta\tau_2$, and T_e dependencies on the applied mw power at $\mathbf{B}=0$. For $\gamma\tau_1$ dependencies: $\gamma_0=10^{-4}\,\mathrm{cm^3\,s^{-1}}$ (solid line), $\gamma_0=10^{-5}\,\mathrm{cm^3\,s^{-1}}$ (dashed line), and $\gamma_0=10^{-6}\,\mathrm{cm^3\,s^{-1}}$ (dotted line) at $\tau_1=10^{-7}$ s. For $\beta\tau_2$ dependencies: $\beta_0=10^{-4}\,\mathrm{cm^3\,s^{-1}}$ (solid line), $\beta_0=10^{-5}\,\mathrm{cm^3\,s^{-1}}$ (dashed line), and $\beta_0=10^{-6}\,\mathrm{cm^3\,s^{-1}}$ (dotted line) at $\tau_2=5\times10^{-9}$ s.

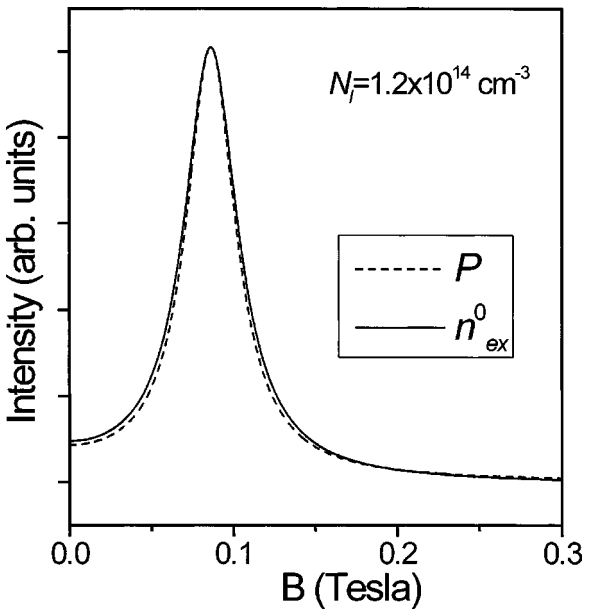

FIG. 6. The calculated CR spectra [given by $P(B)$] and ODCR spectra [given by $|n^0_{\mathrm{ex}}|(B)$] for $N_I=1.2\times10^{14}\,\mathrm{cm^{-3}}$, $T_L=2$ K, and $G=10^{19}$ photons/cm^3 s (using model parameters of Table I). Both resonances show essentially the same linewidth.

Substituting the $T_e(B,P_{\mathrm{mw}})$ dependence of Eq. (5) into the expressions for β and γ in Eq. (2), we obtain a direct dependence of n^0_{ex} on the applied P_{mw} and $\mathbf{B}$. The relative importance of the exciton impact ionization and exciton formation processes in the exciton density modulation under applied mw and magnetic fields can be understood from an analysis of Eq. (2). Using parameters of Table I and $G\sim10^{20}$ photons/cm^3 s, we obtain $\beta\tau_1\tau_2G\ll1$ at $T_e<20$ K in the expression for C_1. Thus the consequential β and γ contributions are included only in the expression for C_2 and therefore are weighted as $\gamma\tau_1+\beta\tau_2$. From Fig. 5, which shows the calculated $\gamma\tau_1$ and $\beta\tau_2$ dependencies on the incident mw power, one can see that $\gamma\tau_1\gg\beta\tau_2$ at low P_{mw} ($P_{\mathrm{mw}}<20$ mW, $T_e<12$ K) for reasonable γ_0 and β_0 values. Using $\gamma_0=10^{-5}\,\mathrm{cm^3s^{-1}}$, we obtain a good agreement between the experimentally observed PL quenching at the applied mw irradiation and the model calculations [$n^0_{\mathrm{ex}}(P_{\mathrm{mw}})$], as shown by the solid line in the inset of Fig. 2. The effect of the exciton impact ionization is important only at high photoexcitation and mw powers. Indeed, the small onset of the exciton impact ionization was observed only at essential electron heating ($T_e>10$ K) and exceedingly strong impact ionization rate ($\beta_0=3\times10^4\,\mathrm{cm^3\,s^{-1}}$), as shown by dotted line in the inset of Fig. 2, in agreement with previous GaAs study.[22] Thus the exciton formation dependence on the hot-electron temperature is a dominant mechanism of the PL modulation at relatively weak mw irradiation.

The magnetic-field dependence of n^0_{ex} exhibits a resonancelike quenching at the CR conditions. Figure 3(b) shows the absolute modulation of the n^0_{ex} value (calculated using the model parameters of Table I) shown by the solid line for $N_I=1.5\times10^{13}\,\mathrm{cm^{-3}}$ and $3\times10^{13}\,\mathrm{cm^{-3}}$ at $P_{\mathrm{mw}}=10\,\mu$W. For comparison, the corresponding magnetic-field dependencies of P [given by Eq. (4)] are also shown in Fig. 3(b) by dashed lines. [Note that since the PMA signal is $\sim n^0P$, where n^0 is the steady-state solution of Eq. (1) for the electron density, the n^0P dependence on the magnetic field is more appropriate to describe the CR trace than the bare P dependence of Eq. (4). However, we do not distinguish between the P and n^0P dependencies, since their line shapes are, in essence, the same at the same set of model parameters.] Therefore the n^0_{ex} and P dependencies on the magnetic-field strength simulate the expected ODCR and CR spectra, respectively. One can see from Fig. 3(b) that the $|n^0_{\mathrm{ex}}|(B)$ resonance linewidth is larger than that of the $P(B)$ resonance. The calculated differences between the $|n^0_{\mathrm{ex}}|(B)$ and $P(B)$ linewidths are similar to the experimentally observed differences between the ODCR and CR line shapes [Fig. 3(a)].

The calculated n^0_{ex} dependence on the applied magnetic field is very sensitive to the residual impurity concentration. Indeed, the $|n^0_{\mathrm{ex}}|$ resonance linewidth is much larger for $N_I=3\times10^{13}\,\mathrm{cm^{-3}}$ than for $N_I=1.5\times10^{13}\,\mathrm{cm^{-3}}$ [see Fig. 3(b)]. It is important to note here that the relative difference between $|n^0_{\mathrm{ex}}|(B)$ and $P(B)$ linewidths reduces as N_I increases. Figure 6 shows the $|n^0_{\mathrm{ex}}|(B)$ and $P(B)$ dependencies for $N_I=1.2\times10^{14}\,\mathrm{cm^{-3}}$ [the rest of the parameters used is the same as in Fig. 3(b)]. One can see that the resonance linewidths are essentially the same. This tendency excuses in some extent the use of the ODCR technique at mw and FIR frequencies to study semiconductors with relatively low mobility. It should be noted, however, that the applicability of our model to FIR CR and ODCR should be considered with caution because high magnetic fields affect carrier mobility and thus the distribution function of hot carriers.[20]

In conclusion, we conducted a comparative study of microwave CR and ODCR spectra in photoexcited undoped GaAs at low temperatures. We found that the ODCR spectrum is broader than the CR spectrum under the same experimental conditions, and thus it does not provide a reliable estimate of the carrier mobility. This unreliability is due to the basic difference between the CR and ODCR methods: while the CR signal is a direct measure of the electric-field

absorption, ODCR results from the combination of T_e dependence on the magnetic-field strength and the hot-electron effect on the exciton formation processes. In order to analyze quantitatively the CR and ODCR spectra, a rate equation model for the exciton and electron densities was used. The model calculations explain well the PL modulation in the microwave and magnetic fields in terms of exciton formation dependence on the hot-electron temperature.

ACKNOWLEDGMENTS

The experimental work at Technion-Israel Institute of Technology was done in the Barbara and Norman Seiden Center for Advanced Electronics. The author would like to express his gratitude to Professor Elisha Cohen, Professor Boris Ashkinadze, and Professor Arza Ron for their encouragement in the field of magneto-optics in semiconductors.

[1] M. G. Wright, A. Kanaah, B. C. Cavenett, G. R. Johnson, and S. T. Davey, Semicond. Sci. Technol. **4**, 590 (1989).
[2] A. Moll, C. Wetzel, B. K. Meyer, P. Omling, and F. Scholz, Phys. Rev. B **45**, 1504 (1992).
[3] M. Godlewski, W. M. Chen, and B. Monemar, CRC Crit. Rev. Solid State Mater. Sci. **19**, 241 (1994).
[4] J. G. Michels, R. J. Warburton, R. J. Nicholas, and C. R. Stanley, Semicond. Sci. Technol. **9**, 198 (1994).
[5] N. T. Son, W. M. Chen, O. Kordina, A. O. Konstantinov, B. Monemar, E. Janzen, D. M. Hofman, D. Volm, M. Drechsler, and B. K. Meyer, Appl. Phys. Lett. **66**, 1074 (1995).
[6] R. J. Warburton, J. G. Michels, R. J. Nicholas, J. J. Harris, and C. T. Foxon, Phys. Rev. B **46**, 13 394 (1992).
[7] D. M. Hofmann, M. Drechsler, C. Wetzel, B. K. Meyer, F. Hirler, R. Strenz, G. Abstreiter, G. Böhm, and G. Weimann, Phys. Rev. B **52**, 11 313 (1995).
[8] Y. T. Dai, Y. F. Chen, and I. Lo, Phys. Rev. B **55**, 5235 (1997).
[9] B. J. H. Liesert, M. Godlewski, A. Stapor, T. Gregorkiewicz, C. A. J. Ammerlaan, J. Weber, M. Moser, and F. Scholz, Appl. Phys. Lett. **58**, 2237 (1991).
[10] Y. T. Dai, Y. H. Chang, T. F. Lee, Y. F. Chen, F. F. Fang, and W. I. Wang, J. Phys. D **26**, 3089 (1996).
[11] J. X. Chen, Y. Oka, C. Y. Hu, W. Ossau, G. Landwehr, K.-J. Friedland, R. Hey, K. Ploog, and G. Weimann, Phys. Rev. B **59**, 8093 (1999).
[12] Y. F. Chen, J. L. Shen, Y. D. Dai, and F. F. Fang, Phys. Rev. B **52**, 4692 (1995).
[13] Y. F. Chen, J. L. Shen, Y. D. Dai, G. J. Jan, and H. H. Lin, Appl. Phys. Lett. **66**, 2543 (1995).
[14] J. L. Shen, Y. D. Dai, Y. F. Chen, S. Z. Chang, and S. C. Lee, Phys. Rev. B **51**, 17 648 (1995).
[15] M. Drechsler, B. K. Meyer, D. M. Hofmann, P. Ruppert, and D. Hommel, Appl. Phys. Lett. **71**, 1116 (1997).
[16] Y. F. Chen, Y. T. Dai, J. C. Fan, T. L. Lee, and H. H. Lin, Appl. Phys. Lett. **67**, 1256 (1995).
[17] W. M. Chen, B. Monemar, E. Sorman, P. O. Holtz, M. Sundaram, J. L. Merz, and A. C. Gossard, Semicond. Sci. Technol. **7**, B253 (1992).
[18] M. Kozhevnikov, E. Cohen, A. Ron, H. Shtrikman, and L. N. Pfeiffer, Phys. Rev. B **56**, 2044 (1997).
[19] V. K. Arora and H. N. Spector, Phys. Status Solidi B **94**, 701 (1989).
[20] Q. X. Zhao, H. Weman, and B. Monemar, Phys. Rev. B **38**, 8529 (1988).
[21] M. Godlewski, T. Lundstrom, Q. X. Zhao, W. M. Chen, P. O. Holtz, and B. Monemar, Phys. Rev. B **52**, 14 688 (1995).
[22] B. M. Ashkinadze, V. V. Bel'kov, and A. G. Krasinskaya, Fiz. Tekh. Poluprovodn. **24**, 883 (1990) [Sov. Phys. Semicond. **24**, 555 (1990)].
[23] J. Cerne, A. G. Markelz, M. S. Sherwin, S. J. Allen, M. Sundaram, A. C. Gossard, P. C. van Son, and D. Bimberg, Phys. Rev. B **51**, 5253 (1995).
[24] R. Romestain and C. Weisbuch, Phys. Rev. Lett. **45**, 2067 (1980).
[25] M. Kozhevnikov, B. M. Ashkinadze, E. Cohen, and A. Ron, Phys. Rev. B **52**, 17 165 (1995).
[26] M. Kozhevnikov, E. Cohen, A. Ron, and H. Shtrikman, Phys. Rev. B **60**, 16 885 (1999).
[27] S. Permagorov, in *Excitons*, edited by E. I. Rashba and M. D. Sturge (North-Holland, Amsterdam, 1982), p. 177.
[28] M. Kozhevnikov, B. M. Ashkinadze, E. Cohen, and A. Ron, Solid State Commun. **106**, 73 (1998).
[29] W. J. Rappel, L. F. Feiner, and M. F. H. Schuurmans, Phys. Rev. B **38**, 7874 (1988).
[30] B. M. Ashkinadze and A. V. Subashiev, Pis'ma Zh. Eksp. Teor. Fiz. **46**, 284 (1987) [JETP Lett. **46**, 357 (1987)].
[31] M. Kozhevnikov, B. M. Ashkinadze, E. Cohen, A. Ron, and H. Shtrikman, Phys. Rev. B **60**, 16 894 (1999).
[32] We assume that the electron recombination in bulk GaAs is predominantly radiative via the capture of electrons by ionized donors. Taking this capture cross section $\sigma \sim 5\times10^{-15}\,\mathrm{cm}^2$ [D. Bimberg, H. Munzel, A. Steckenborn and J. Christen, Phys. Rev. B **31**, 7788 (1985)], donor concentration $N_D \sim 2\times10^{13}\,\mathrm{cm}^{-3}$ and $v_e \sim 2\times10^6$ cm/s at $T_L = 2$ K, we obtain $\tau_1 = \sigma \nu_e N_D \sim 2\times10^{-6}$ s.
[33] G. W. 't Hooft, W. A. J. van der Poel, and L. W. Molenkamp, Phys. Rev. B **35**, 8281 (1987).
[34] M. Gurioli, P. Borri, M. Colocci, M. Gulia, F. Rossi, E. Molinari, and P. E. Selbmann, Phys. Rev. B **58**, R13 403 (1998).
[35] $\beta_0 = \pi a_B^2 v_e$, using $a_B \sim 120$ Å and $v_e \sim 3\times10^6$ cm/s at $T_L = 2$ K.
[36] Using the exctitation density $n_e \sim 10^{14}\,\mathrm{cm}^{-3}$ and the PL rise time $t_f \sim 200$ ps at the resonance excitation (we adopt the PL rise time to be equal to the exciton formation time) from Ref. 34, we obtain $\gamma_0 = (n_e t_f)^{-1} \sim 5\times10^{-5}\,\mathrm{cm}^3\,\mathrm{s}^{-1}$.
[37] B. K. Ridley, Phys. Rev. B **41**, 12 190 (1990).
[38] G. E. Stillman, S. S. Bose, M. H. Kim, B. Lee, and T. S. Low, in *Handbook on Semiconductors*, edited by S. Mahajan (North-Holland, Amsterdam, 1994), Vol. 3a, p. 940.
[39] R. Ulbrich, Phys. Rev. B **8**, 5719 (1973).
[40] C. Piermarocchi, F. Tassone, V. Savona, A. Quattropani, and P. Schwendimann, Phys. Rev. B **55**, 1333 (1997).
[41] C. Piermarocchi, V. Savona, A. Quattropani, P. Schwendimann, and F. Tassone, Phys. Status Solidi B **204**, 191 (1997).
[42] K. Seeger, *Semiconductor Physics*, 6th ed. (Springer-Verlag, Berlin, 1997), p. 106.
[43] K. Seeger, *Semiconductor Physics* (Ref. 42), p. 379
[44] K. W. Boer, *Survey of Semiconductor Physics* (Van Nostrand Reinhold, New York, 1990), p. 747.
[45] P. Lorrain and D. R. Corson, *Electronagnetic Fields and Waves* (W. H. Freeman and Company, San Francisco, 1970), Chap. 13.